*J. Fluid Mech.* (1978), *vol.* 86, *part* 3, *pp.* 513–543
*Printed in Great Britain*



# Statistical features of heat transfer in grid-generated turbulence: constant-gradient case

By K. S. VENKATARAMANI† AND R. CHEVRAY
Department of Mechanical Engineering, State University of New York, Stony Brook

(Received 19 July 1977)

Turbulence produced by a grid which simultaneously imparts a mean temperature profile varying linearly with height was investigated in a specially constructed wind tunnel. While the mean temperature profile is preserved downstream of the grid in accordance with the theory of Corrsin (1952), the downstream evolution of the r.m.s. temperature fluctuation is at variance with his prediction. The reason for this discrepancy is shown to lie in the neglect of molecular diffusivity, which leads to unbounded growth of the fluctuations. Along with conventional correlations and spectra, the filtered heat-transfer correlation is presented. About 60 % of the heat transport is accomplished by the low wavenumber components having length scales equal to or larger than the integral scale. An intriguing feature of the present experiments is the presence of an inertial–convective subrange for the temperature field notwithstanding the low Reynolds number and the consequent absence of an inertial subrange for the velocity field. Experimental results show that the temperature has a positive skewness everywhere in contrast to the velocity components, which are symmetrically distributed. Measurements of the joint probability density function of the vertical component of the velocity and the temperature indicate that, while the assumption of joint normality is not uniformly valid, the conditional expectations nearly follow the normal law. Marginal and joint moments of up to fourth order are presented. Odd-order joint moments are clearly sensitive to the skewness of the temperature.

## 1. Introduction

The study of turbulent diffusion began with the pioneering work of Taylor (1921), who studied the dispersion of fluid particles in a homogeneous turbulence with zero velocity. Corrsin (1952) made use of these findings to investigate the problem of an isotropic turbulence on which a mean temperature profile varying linearly with height was imposed at some plane normal to the mean flow direction. He arrived at the remarkable result that the mean temperature profile continued to be linear with the same slope downstream of the plane where it was introduced. His theory received its first experimental scrutiny in the work of Wiskind (1952), who confirmed the prediction about the mean temperature profile downstream of the heated grid imposing the temperature profile. Wiskind did not, however, fully examine the joint statistics of the velocity and temperature fields. Recently, in the course of investigating the wake of a cylinder in a stratified flow, Alexopoulous & Keffer (1971) repeated some of Wiskind's measurements and reconfirmed the prediction about the evolution of the mean tem-

† Present address: General Applied Science Laboratory, Westbury, New York 11590.

perature profile. Here we are interested in examining the assumptions made by Corrsin and their possible consequences and in furthering the experiments of Wiskind and Alexopoulous & Keffer, which, while providing some interesting results and a measure of confidence in the approach of the theory, left many related questions unanswered. In particular, since any statistical approach to the problem of heat transport by the random velocity field has at its heart the joint probability structure of the velocity and temperature fields, some emphasis has been laid upon the joint probability density functions and moments of the velocity and temperature.

## 2. Discussion of Corrsin's theory

Corrsin's work on homogeneous turbulence with a linearly varying mean temperature profile represents a significant achievement in posing a conceptually simple problem in turbulent transport and obtaining useful results from it. It is of interest to examine the assumptions made in the theory and their consequences. Corrsin (1952) considered the case of a distributed heat source in a given plane normal to the mean velocity in a non-decaying homogeneous turbulence with mean velocity $\overline{\mathbf{U}} = i\mathbf{U}$. The absolute temperature $\overline{T}_0$ at the source plane (say $x = 0$) was taken to be a linear function of the vertical co-ordinate $z$:

$$\overline{T}_0 = \overline{T}_1 + \frac{d\overline{T}_0}{dz} dz. \tag{1}$$

From the similarity of the mean thermal wake of a line source and by making use of the linearity of the diffusion equation to superpose the mean temperature fields of many sources, Corrsin obtained in the limit of a distributed source

$$\overline{T}(x, z) = \overline{T}_1 + \frac{d\overline{T}_0}{dz} dz, \tag{2}$$

which states that the mean temperature for this problem is independent of $x$.

While considering the temperature fluctuations, his analysis was restricted to the case of zero molecular diffusivity. With this assumption, the dispersion (mean-squared displacement) of heat is obviously the same as that of fluid particles. He set up a 'reversed diffusion by continuous movements' in which he considered the previous dispersion of fluid particles which later passed through a given Eulerian location instead of considering the dispersion of all particles which originally passed through a fixed point. The validity of this approach was rigorously established by him in a later study (Corrsin 1972). Using Taylor's (1921) result for the dispersion of fluid particles in a homogeneous turbulence, he arrived at

$$\theta'(x) = \left\{ 2 \frac{\overline{w^2}}{\overline{U}^2} \int_0^x (x - \xi) R_{wL}(\xi) \, d\xi \right\}^{\frac{1}{2}} \frac{d\overline{T}}{dz}, \tag{3}$$

where $\theta'$ is the r.m.s. temperature fluctuation and $R_{wL}(\xi)$ is the Lagrangian 'spatial' autocorrelation coefficient defined by

$$R_{wL}(\xi) = \langle w(x) \, w(x + \xi) \rangle / \overline{w^2}. \tag{4}$$

It can be seen from (3) that for $x \to 0$

$$\theta'(x) = \frac{w'}{\overline{U}} \frac{d\overline{T}}{dz} x \tag{5}$$

and for $x \to \infty$

$$\theta'(x) = \frac{w'}{\overline{U}} \frac{d\overline{T}}{dz} (2\mathscr{L}x)^{\frac{1}{2}}, \tag{6}$$

where

$$\mathscr{L} = \int_0^\infty R_{wL}(\xi)\, d\xi, \tag{7}$$

the Lagrangian integral length scale.

Equation (6) clearly depicts the serious shortcoming of the assumption of zero molecular diffusivity for, according to (6), the r.m.s. temperature fluctuation will grow indefinitely with $x$.

Using Taylor's dispersion result, the rate of heat transport by turbulence

$$\dot{Q} = \rho C_p \langle \theta w \rangle$$

becomes

$$\dot{Q} = -\rho C_p \frac{\langle w^2 \rangle}{\overline{U}} \frac{d\overline{T}}{dz} \int_0^x R_w(\xi)\, d\xi, \tag{8}$$

which in the limit $x \to 0$ gives

$$\dot{Q} = -\rho C_p \frac{\langle w^2 \rangle}{\overline{U}} \frac{d\overline{T}}{dz} x \tag{9}$$

and in the limit $x \to \infty$ gives

$$\dot{Q} = -\rho C_p \frac{\langle w^2 \rangle}{\overline{U}} \frac{d\overline{T}}{dz} \mathscr{L}, \tag{10}$$

which is independent of position. However, the heat-transfer correlation coefficient, defined as

$$R_{\theta w} = \langle \theta w \rangle / \theta' w', \tag{11}$$

decreases monotonically with $x$ (owing to the monotonic increase in $\theta'$ with $x$), giving the following asymptotic values:

$$R_{\theta w} = \begin{cases} -1 & (x \to 0), \\ 0 & (x \to \infty). \end{cases} \tag{12}$$

As already mentioned, the neglect of molecular diffusivity leads to an unbounded growth of $\theta'$ with $x$. This is reflected directly in the downstream evolution of the heat-transfer correlation coefficient. In fact, Corrsin remarked that molecular diffusivity would have to be included to obtain a non-zero asymptote for $R_{\theta w}$. When we modify the analysis by including the molecular diffusivity we can see qualitatively the changes in the results. These come about in two ways. On the one hand, the dispersion of heat is different from that of fluid particles, and on the other, a fluid particle does not retain the same value of the temperature along its trajectory since the effect of molecular diffusivity is to change it. The first aspect has been considered by Saffman (1960), Okubo (1967) and Chevray & Venkataramani (1977). From these studies, the total dispersion of heat is found to be less than the sum of the individual dispersions due to the turbulent and direct molecular diffusion processes.

In the Lagrangian description which is appropriate for this problem, the diffusion equation reads

$$\frac{\partial\theta(\mathbf{a},t)}{\partial t} = \alpha J\left\{\frac{J,x_2,x_3}{a_1,a_2,a_3}\right\} + \alpha J\left\{\frac{x_1,J,x_2}{a_1,a_2,a_3}\right\} + \alpha J\left\{\frac{x_1,x_2,J}{a_1,a_2,a_3}\right\}, \tag{13}$$

where $\mathbf{a}$ denotes the initial (at time $t = 0$, say) co-ordinates (in a fixed frame of reference) of a fluid particle that arrives at the position $\mathbf{x}$ at time $t$, $\alpha$ is the molecular diffusivity and $J$ is the Jacobian of the transformation. Expanding the Jacobian we obtain

$$\begin{aligned}\frac{\partial\theta(\mathbf{a},t)}{\partial t} = \alpha\Bigg\{&\left[\frac{\partial^2\theta}{\partial a_1^2}\left(\frac{\partial x^2}{\partial a_2}\frac{\partial x_3}{\partial a_3} - \frac{\partial x_2}{\partial a_3}\frac{\partial x_3}{\partial a_2}\right) + \frac{\partial\theta}{\partial a_1}\frac{\partial x_3}{\partial a_3}\frac{\partial^2 x_3}{\partial a_1\,\partial a_2}\right.\\ &\left. + \frac{\partial\theta}{\partial a_1}\frac{\partial x_2}{\partial a_2}\frac{\partial^2 x_3}{\partial a_1\,\partial a_3} - \frac{\partial\theta}{\partial a_1}\frac{\partial x_3}{\partial a_2}\frac{\partial^2 x_3}{\partial a_1\,\partial a_3} - \frac{\partial\theta}{\partial a_1}\frac{\partial x_2}{\partial a_3}\frac{\partial^2 x_3}{\partial a_1\,\partial a_3}\right]\\ &- \left[\frac{\partial^2\theta}{\partial a_2^2}(\ldots) + \ldots\right] + \left[\frac{\partial^2\theta}{\partial a_3^2}(\ldots) + \ldots\right]\Bigg\}\\ &\times\alpha\{[\ldots] + \ldots\} + \alpha\{[\ldots] + \ldots\}.\end{aligned} \tag{14}$$

Equation (14) makes it clear that an evaluation of the temperature history of the fluid particle is immensely difficult owing to the rather awkward moments which the terms on the right-hand side (one of which is written explicitly) will introduce even when one is interested in the evolution of a low-order statistical quantity like the r.m.s. temperature fluctuation.

On the other hand, if we consider the Eulerian diffusion equation we can reach some tangible conclusions. Although this equation does not lend itself to a closed-form solution (as is well known), we can still attempt a cavalier approach and make a series of assumptions using physical reasoning as a guide. The equation for the mean-squared temperature fluctuations in the Eulerian frame of reference is

$$\frac{\partial\langle\theta^2\rangle}{\partial t} + U_j\frac{\partial\langle\theta^2\rangle}{\partial x_j} = -2\langle u_j\theta\rangle\frac{\partial\Theta}{\partial x_j} - \frac{\partial}{\partial x_j}\langle u_j\theta^2\rangle + \alpha\frac{\partial^2}{\partial x_j\,\partial x_j}\langle\theta^2\rangle - 2\alpha\left\langle\frac{\partial\theta}{\partial x_j}\frac{\partial\theta}{\partial x_j}\right\rangle. \tag{15}$$

For a steady case, the first term on the left-hand side of (15) is zero. Furthermore, when the mean velocity is given by

$$U_j = U\delta_{j1} \tag{16}$$

the second term on the left side reduces to

$$Ud\langle\theta^2\rangle/dx.$$

Since, as in Corrsin's work, a mean temperature gradient exists only in the $x_3$ direction, the first term on the right side is

$$-2\langle\theta u_3\rangle\,\partial\Theta/\partial x_3.$$

Hence (15) can be written as

$$U\frac{d\langle\theta^2\rangle}{dx_1} = \underset{①}{-2\langle\theta u_3\rangle\frac{\partial\Theta}{\partial x_3}} \underset{②}{-\frac{\partial}{\partial x_j}\langle u_j\theta^2\rangle} \underset{③}{+\alpha\frac{\partial^2\langle\theta^2\rangle}{\partial x_j\,\partial x_j}} \underset{④}{-2\alpha\left\langle\frac{\partial\Theta}{\partial x_j}\frac{\partial\Theta}{\partial x_j}\right\rangle}. \tag{17}$$

Looking now at the right-hand side of (17), the term ① is the production term (of temperature fluctuations) due to the action of the turbulence on the mean temperature gradient, ② is due to the convection of $\theta^2$ by turbulence, ③ is the molecular diffusion term and ④ describes the destruction of the temperature fluctuations by the action of the molecular diffusivity.

We may argue that the second and third terms will be small compared with the production term in an approximately homogeneous temperature field. Using local isotropy, the last term, denoting the destruction, can be written as

$$-12\alpha\langle\theta^2\rangle/\lambda_\theta^2,$$

where $\lambda_\theta$ is the Corrsin microscale of the temperature fluctuations (Corrsin 1951*a*; 1952). We should expect the production term to attain a constant asymptotic value as $x_1 \to \infty$. According to (10), which was derived under the restrictive assumption of zero molecular diffusivity, this is so. It then appears that the success of (10) in predicting the correct asymptotic behaviour despite the neglect of molecular diffusivity is due to the fact that the turbulent transport of heat is most efficiently carried out by the large-scale eddies while molecular diffusivity is most effective in smearing out the temperature differences in the small scales. Equation (10) should then lead to the correct behaviour since the neglected molecular diffusivity becomes of minor importance. Hence (17) can be reduced to a linear first-order ordinary differential equation:

$$U d\langle\theta^2\rangle/dx_1 + 12\alpha\langle\theta^2\rangle/\lambda_\theta^2 = P, \tag{18}$$

where $P$ denotes the production term and the solution of this equation is

$$\langle\theta^2\rangle = c\exp\left\{-\frac{12\alpha}{\lambda_\theta^2\overline{U}}x_1\right\} + 2\frac{\langle w^2\rangle}{\overline{U}}\left(\frac{d\Theta}{dx_3}\right)^2\exp-\left\{\frac{12\alpha}{\lambda_\theta^2\overline{U}}\right\}\int_0^{x_1}\frac{\lambda_\theta^2 U}{12\alpha}$$
$$\times\left\{\exp\left(\frac{12\alpha}{\lambda_\theta^2\overline{U}}x_1\right) - \exp\left(\frac{12\alpha}{\lambda_\theta^2\overline{U}}y\right)\right\}R_w(y)\,dy. \tag{19}$$

The expression for $P$ is taken from (8) and $\lambda_\theta$ is assumed to be constant. The asymptotic result for $x_1 \to \infty$ obtained from (19) is identical with the solution obtained by treating $P$ as a constant. Equation (19) shows that for large values of $x_1$ the mean-squared temperature fluctuations decay with increasing $x_1$, a result we should expect on physical grounds.

A less fundamental but nevertheless important point when comparing laboratory experiments with Corrsin's theory is the assumption of a non-decaying turbulence field, which is obviously untenable even in the approximately homogeneous turbulence behind a grid. Another significant departure from the theory encountered in a laboratory simulation is that the heated grid which is the counterpart of the theory's source plane introduces not only a mean temperature gradient but also temperature fluctuations about the mean. A fluid particle leaving the grid plane and arriving at any downstream location therefore brings with it a temperature perturbation about the local mean not only because the mean temperature acquired at the source plane is different from that at the new position which the fluid particle has reached (the process considered by Corrsin) but also because the fluid particle has simultaneously acquired a fluctuation about the mean temperature at the grid plane.

## 3. Experimental set-up, acquisition and processing of data

In order to investigate experimentally the velocity and temperature fields in a nearly homogeneous, grid-generated turbulence with a specified mean temperature profile in the vertical direction, a low-speed wind tunnel was designed and constructed and is described in detail by Venkataramani (1977) and Venkataramani & Chevray (1977). The free-stream turbulence intensity was less than 0·12 % over the part of the test section where the measurements were made. The heater section of the wind tunnel served a dual purpose: housing the heaters and providing the turbulence-generating biplanar grid. This grid consisted of the horizontal heater elements and vertical metal rods of the same diameter. The heater elements (diameter = $\frac{3}{8}$ in., heated length = 11 in., maximum rating = 450 W; manufactured by Hotwatt, Inc.) were quartz tubes each containing a Nichrome filament. All the experiments reported in this investigation were conducted using eleven heaters with a corresponding mesh length of 1·5 in. The test section consisted of a rectangular duct of length 8 ft and inside dimensions 16 in. (height) × 11 in. (width). To minimize the heat loss from the walls, fibreglass insulation was wrapped around the test section.

Simultaneous measurements of velocity and temperature were made with an analog instrument developed by Chevray & Tutu (1972). It comprised two hot-wire probes, the leading wire being operated as a resistance thermometer, providing a signal proportional to the temperature, and the second wire being operated in the constant-temperature mode, yielding a signal with contributions from both temperature and velocity. The signal from the second wire was dynamically compensated for the effects of the variation of fluid temperature and the consequent variation of fluid properties through a linearizer. A signal varying linearly with the velocity was thus generated. This technique was extended to the cross-wire configuration so that simultaneous and continuous signals for two velocity components ($u$ and $w$) and the temperature were obtained.

Three hot-wire sensors were used to generate simultaneously the $u$, $w$ and $\theta$ signals. The leading sensor, made of Wollaston wire (Pt–Rh; 10 % Rh), was mounted on to a standard DISA 55A32 X-probe by using a collar machined to fit the conical taper of the X-probe; the Wollaston wire was spot welded onto its prongs. The etched portion of the wire had a diameter of 0·635 $\mu$m and a typical length of the order of 2·0 mm, corresponding to a resistance of about 1000 $\Omega$ at room temperature. A modified (for use with large resistance sensors) Flow Corporation 1900–1 constant-current anemometer was used to operate this Wollaston wire as a resistance thermometer with a current of 120 $\mu$A. At this low current the velocity sensitivity of the wire is given by Wyngaard (1971) to be 0·006 °C/($m^{-1}$ s) but direct measurements gave 0·009 °C/($ms^{-1}$). Frequency compensation of the temperature signal was dispensed with since the frequency response was good up to 6·4 kHz for the worst condition of zero velocity (Tutu 1976). All other wires were made of tungsten (3·81 $\mu$m in diameter; 1·2 mm long) spot welded onto X-probes and were operated in the constant-temperature mode. Linearization was accomplished simultaneously with the temperature compensation as described by Chevray & Tutu (1972). The linearized and temperature-compensated signals from the constant-temperature anemometers and the signal from the constant-current anemometer were recorded on a magnetic tape using a Honeywell 7610 FM tape recorder equipped with phase lock.

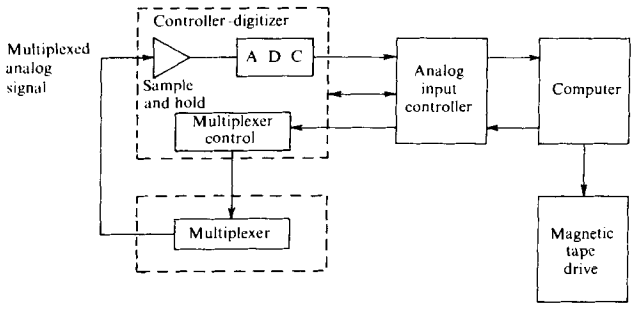


FIGURE 1. Schematic diagram of analog-to-digital conversion.

To obtain time-averaged mean values, a Hewlett-Packard 2212A voltage-to-frequency converter (100000 pulses $s^{-1}$/V) and a modified Hewlett-Packard 5330A preset counter with seven digits and a 100 s gate time were used to perform true integrations. In order to reduce the scatter in the data, integration times of 300 s were found necessary. While performing the r.m.s. measurements, the d.c. voltages were offset, thus eliminating high pass filtering errors inherent in a.c. coupled measurements.

One-dimensional spectra of the velocity components and the temperature were obtained from a Hewlett-Packard 302A wave analyser with a bandwidth of 6 Hz while time-delayed auto- and cross-correlations together with probability density functions of the signals were measured with a Hewlett-Packard 3721A correlator operated in the d.c. coupled mode. Two different methods were employed to measure the filtered correlation of $w$ and $\theta$. In the first, two identical wave analysers set at the same centre-frequency were used and in the second a single wave analyser was used to measure separately the spectra of $w+\theta$ and $w-\theta$, from which the filtered correlation was computed. The tape recorder was played back 16 times faster in both cases in order to extend the frequency range of the wave analyser to lower values.

Processing of most of the data was accomplished by playing back the tape recorder, multiplexing the signals, sampling these digital values with a computer at a constant rate and then writing them on a magnetic tape in the multiplexed mode. A schematic sketch of the set-up for the analog-to-digital conversion is shown in figure 1. The entire process was under the control of a PDP 15 digital computer. The played-back signals from the tape recorder were multiplexed by a Scientific Data Systems MR50 analog multiplexer and fed to an SDS CD51 controller digitizer (with 14 data bits and one sign bit) which performed the conversion and returned the digital values. The multiplexer was controlled by the digitizer, which in turn was controlled by an SDS 7915 analog input controller. Commands from the computer were transmitted to the input controller and the digital values returned by the digitizer transferred to the computer memory. A Digital Equipment Corporation tape drive was used for writing the numerical values on a magnetic tape.

In order to avoid loss of samples during the interval between the data acquisition by the computer and the transfer to the tape, the software was modified to incorporate two buffers in the computer memory. When one of them acquired the data, the other performed the transfer. After the writing had been completed, the buffers were then interchanged and this ensured recovery of all the data. The software was written to handle four analog channels. Thus the two linearizer output signals, the temperature

signal and a periodic timing signal could be digitized simultaneously. The numbers were written in blocks of one-thousand, corresponding to 250 values for each of the channels. Owing to storage limitations of the computer and the transfer speed of the data, the signals had to be played back 16 times slower than the speed at which they were recorded. The real-time values of the sampling frequency and the multiplexing interval were $20{\cdot}8 \times 10^3$ samples $s^{-1}$/channel and 4·25 $\mu$s, respectively. The upper acquisition frequency of this system is 10·4 kHz, which from the Nyquist criterion is more than adequate for our purposes. The magnetic tape containing the numerical values was run on a Univac Uniservo 9 tape drive and the information transferred to the core of a Univac 1110 time-sharing digital computer for the final computations by the use of a fast tape-to-core transfer. For each measuring station, the total number of samples was typically $2 \times 10^6$ ($5 \times 10^5$ for each of the four channels: two linearizer output signals, the temperature signal and the timing signal).

## 4. Experimental results and discussion

While the closest laboratory simulation of the theoretical concept of isotropic turbulence is achieved downstream of a grid, it has been well established (Grant & Nisbet 1957; Uberoi 1963; Uberoi & Wallis 1966; Comte-Bellot & Corrsin 1966, 1970; Kistler & Vrebalovich 1966) that grid turbulence does not satisfy one of the major requirements of isotropy, namely the equality of the kinetic energies (per unit mass) associated with the longitudinal and transverse components of the turbulent velocity. This is also true in our case as is brought out by figure 2. In this and the following figures $x$ is the distance downstream of the midplane of the grid, $M$ is the mesh length and $z$ is the vertical distance from the horizontal midplane of the test section (positive upwards). At 43·2 mesh lengths downstream of the grid, the ratio of the r.m.s. values of the vertical and longitudinal components of the turbulent velocity has a nearly constant value of 0·861 across the height of the test section. Table 1 shows a comparison of this value with those of other investigators. Obviously, apart from the inhomogeneity in the longitudinal direction introduced by the viscous decay, the grid turbulence departs from isotropy mainly owing to the anisotropy of the large scales. It is nevertheless possible to make grid turbulence isotropic with respect to the kinetic energies by introducing a mean strain rate. Often this is accomplished by having a contraction after the grid. Comte-Bellot & Corrsin (1966, 1970) used a 1·27:1 contraction with success while Uberoi & Wallis (1966) achieved the same result with a 1·25:1 contraction. Unfortunately, we could not employ this method of producing isotropy since the concomitant temperature fluctuations produced by the grid and perhaps also the mean temperature gradient would also be influenced by the secondary contraction. At present, there appears to be no concensus on the return of turbulence towards the initial anisotropy downstream of the contraction. From figure 2 it can be seen that the maximum variation of the r.m.s. velocities from their centre-line values is of the order of 4 %, which is considerably less than the variation in the experiments of Grant & Nisbet for a 1 in. grid.

Figure 3, which depicts the on-line measurements of the mean temperature profiles at various $x/M$ locations, reflects the notable success of the theory in predicting the mean temperature profile to be the same at all $x$ locations downstream of the grid. Measurements of the mean temperature from signals recorded at selected stations

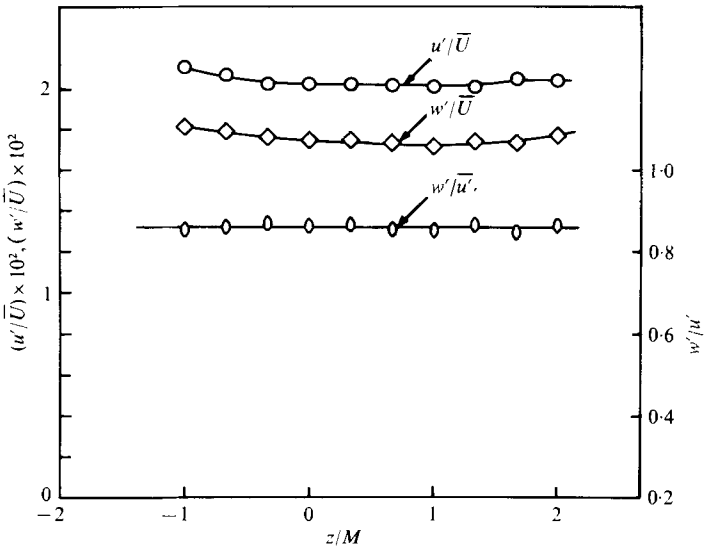


FIGURE 2. R.m.s. velocity components at $x/M = 43{\cdot}2$.

| | References | $v'/u'$ or $w'/u'$ |
|---|---|---|
| 1 | Uberoi & Wallis (1966) (without contraction after grid) | 0·8452 |
| 2 | Grant & Nisbet (1957) | 0·8832 |
| 3 | Kistler & Vrebalovich (1966): | |
| | $Re_L = 1{\cdot}33 \times 10^4$ | 0·8122 |
| | $Re_L = 7{\cdot}5 \times 10^3$ | 0·7767 |
| | $Re_L = 6{\cdot}53 \times 10^3$ | 0·75 |
| | $Re_L = 1{\cdot}54 \times 10^3$ | 0·7114 |
| 4 | Comte-Bellot & Corrsin (1966) (without contraction, biplanar grid) | 0·90–0·96 |
| 5 | Present design | 0·861 |

TABLE 1. Comparison of the ratio of the lateral and longitudinal turbulence intensities in various tunnels.

($x/M = 17{\cdot}7, 43{\cdot}2, 49{\cdot}2, 55{\cdot}2$) are presented in figure 4. Again, these are in conformity with the theory as well as with the measurements reported previously by Wiskind (1962) and Alexopoulos & Keffer (1971). Although Corrsin's theory was originally formulated for a non-decaying homogeneous turbulence it nevertheless seems to work well for a decaying turbulence behind a grid. The probable reason is that, even in a decaying turbulence behind a grid, the thermal wake of a line source displays similarity under some restrictions usually satisfied by experiments. Moreover, the molecular term also obeys similarity as was indicated by Venkataramani (1977), who used the similarity arguments of Tennekes & Lumley (1972, p. 223) to arrive at the conclusion that Corrsin's result for the mean temperature profile holds good in the experiments despite the presence of molecular diffusivity and decay of the turbulence field.

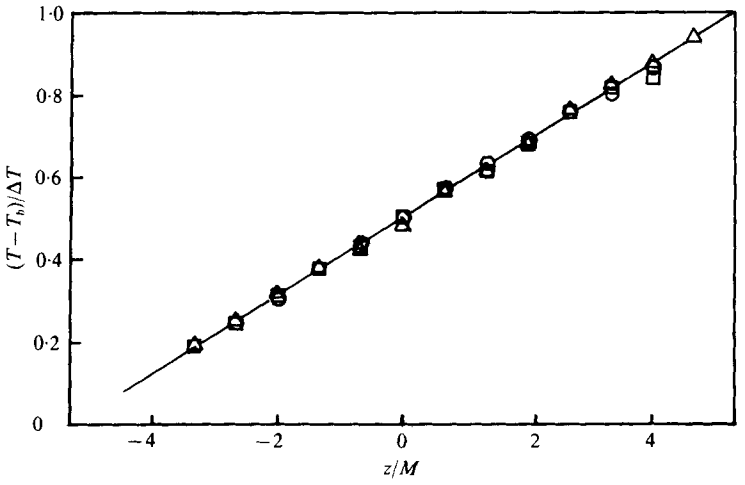


FIGURE 3. On-line measurements of mean temperature profiles. △, $x/M$ = 7·0; □, $x/M$ = 18·1; ○, $x/M$ = 43·6.

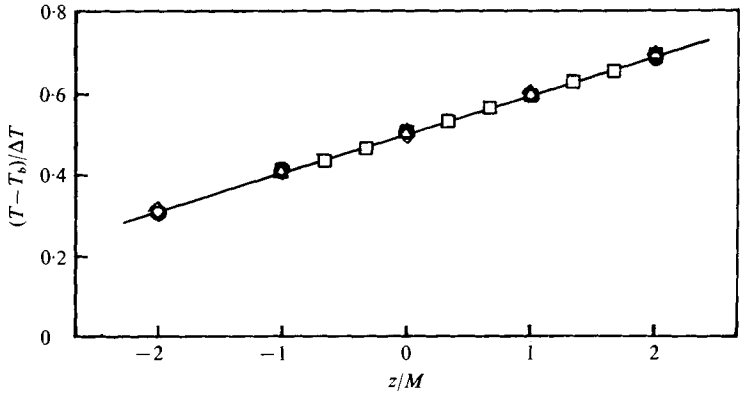


FIGURE 4. Mean temperature profiles for the recorded stations. ○, $x/M$ = 17·7; □, $x/M$ = 43·2; ◇, $x/M$ = 49·2; △, $x/M$ = 55·2.

It may readily be observed in figure 5 that $\theta'$ is not uniform across the height of the test section but generally increases with height. This behaviour was also observed by Wiskind and Alexopoulos & Keffer. They dismissed the possibility that the production of the $\overline{\theta^2}$ stuff (in Batchelor's terminology: Batchelor, Howells & Townsend 1959; Batchelor 1959) is a function of the mean temperature level by analogy with the situation of constant linear velocity gradient, where the production of $\overline{q^2}$ depends only upon $\overline{uv}$ and the constant velocity gradient. They put forth the argument that the flow is still in a developing state as regards the fine-scale structure and it is the balance of production, diffusion and dissipation of the $\overline{\theta^2}$ stuff which is temporarily dependent upon the mean temperature level. An important point pertaining to the non-uniformity of $\theta'$ is that, during the process of creating the mean temperature profile, the heated grid simultaneously gives rise to fluctuations of the temperature about the local mean as was mentioned in § 2. Although in the immediate vicinity of the grid $\theta'$ must be roughly proportional to the mean $\overline{T}$, further downstream of the grid this $\theta'$ distribution can be

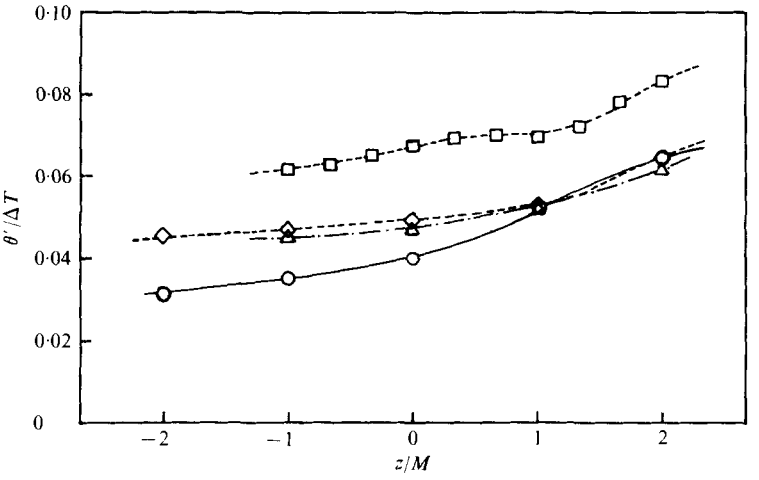


FIGURE 5. R.m.s. temperature profiles. Symbols as in figure 4.

expected to approach homogeneity in the vertical direction, chiefly through the action of the molecular diffusivity. This tendency is revealed in figure 5, where at $x/M = 49{\cdot}2$ and $55{\cdot}2$ the $\theta'$ distribution is nearly uniform. An interesting comparison can be made here with the experiments on a nearly homogeneous turbulent shear flow conducted by Champagne, Harris & Corrsin (1970). Using an array of parallel channels with different resistances they produced a flow whose mean velocity varied linearly with height. Although they obtained a linear mean velocity profile as early as 40 channel heights, the turbulent velocity components displayed non-uniformity up to 102 channel heights. Hence the non-uniformity of $\theta'$ observed in our experiments and those of Wiskind and Alexopoulos & Keffer is to be expected as the conditions are somewhat similar to the uniform-shear case.

Another feature of the $\theta'$ profiles is that from $x/M = 17{\cdot}7$ to $43{\cdot}2$, $\theta'$ increases at all the vertical locations and from then on decreases. The initial increase is in accordance with the theory, which predicts a linear relation between $\overline{\theta^2}$ and the Lagrangian dispersion. A similar increase was present in the two earlier experimental works cited. As for the decrease in $\theta'$ downstream of $x/M = 43{\cdot}2$, a likely reason is the predominance of the molecular destruction of $\overline{\theta^2}$ over the production due to the presence of the mean gradient, which was treated in §2. Earlier studies, however, did not show a definite decrease of $\theta'$ with $x$ even up to $x/M = 172$. Not all the grid geometries used were the same. Ours is geometrically similar (with a solidity of 0·44) to that of Mills *et al.* (1958) and Mills & Corrsin (1959), who studied the decay of the temperature field downstream of a uniformly heated grid. Wiskind used a grid of solidity 0·34 and Alexopoulos & Keffer employed a grid consisting of only horizontal heaters. Furthermore, for a substantial part of his work, Wiskind introduced a secondary, unheated grid at $x/M = 72$. This makes the task of comparison particularly difficult since it is not possible for the secondary grid to alter the turbulent velocity field alone without simultaneously affecting the fluctuating temperature field. If the measurements made with the auxiliary grid are excluded from this comparison, then we can only conclude that the differences in the grid geometry could be of only minor importance in determining the trend of the downstream evolution of $\theta'$. The test section was insulated only

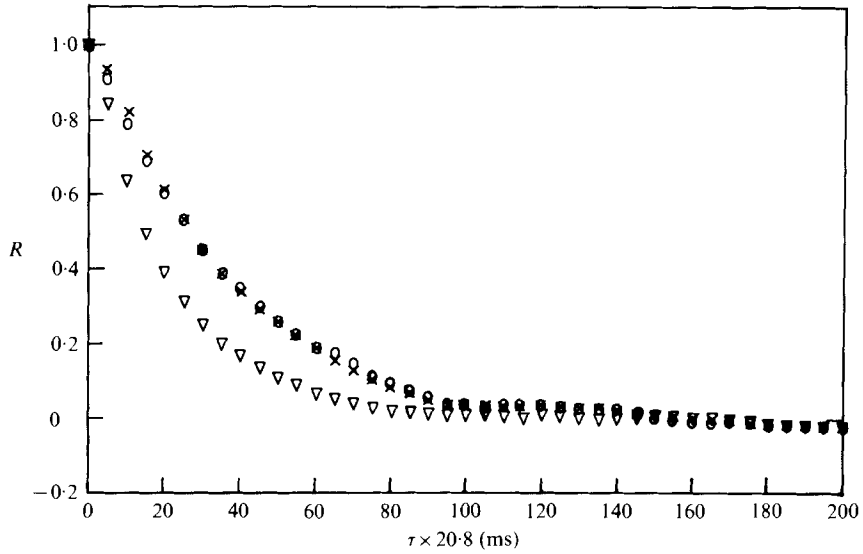


FIGURE 6. Correlation curves. $x/M = 43{\cdot}2$. ○, $R_{\theta\theta}(\tau)$; ▽, $R_{ww}(\tau)$; ×, $R_{w\theta}(\tau)$.

in our experiments; this however could have a significant effect only near the walls of the test section and therefore should not be a major source of discrepancy in the present context. The last and most important difference lies in the value of the mean temperature gradient, which was 0·1 °C/cm in our experiments as compared with 0·25 °C/cm in Wiskind's and 0·22 °C/cm in that of Alexopoulos & Keffer. As the uniform mean temperature gradient lacks an inherent length scale, another criterion must be sought for similarity before the role of the temperature gradient can be assessed. Since the Péclet numbers based on the grid mesh length are of comparable magnitude for all three experiments ($0{\cdot}83 \times 10^4$ for Wiskind, $0{\cdot}59 \times 10^4$ for Alexopoulos & Keffer, $1{\cdot}44 \times 10^4$ for the present study), it is reasonable to conclude that the relative roles of convection and molecular diffusion are nearly the same in all the experiments and hence the magnitude of the mean temperature gradient would play a crucial part in determining the balance of the production of $\overline{\theta^2}$ and its destruction by molecular action. Inasmuch as the mean gradient in this study was less than that in the other two investigations, the departure from the conditions for a uniformly heated grid must also be less. Clearly then, the molecular destruction term should exceed the production term earlier than in the other experiments. This conclusion is consistent with the results of the measurements.

The normalized autocorrelations of the temperature and the vertical component of the velocity, defined by

$$\left.\begin{aligned} R_{\theta\theta}(\tau) &= \langle\theta(t')\,\theta(t'+\tau)\rangle/\overline{\theta^2} \\ \text{and} \quad R_{ww}(\tau) &= \langle w(t')\,w(t'+\tau)\rangle/\overline{w^2}, \end{aligned}\right\} \tag{20}$$

are shown in figure 6. The same figure also contains the normalized cross-correlation of $w$ and $\theta$, defined by

$$R_{w\theta}(\tau) = \langle w(t')\,\theta(t'+\tau)\rangle/\overline{w\theta}. \tag{21}$$

For a given delay $\tau$, $R_{\theta\theta}$ and $R_{w\theta}$ are larger than $R_{ww}$ except at large values of $\tau$, when the normalized correlation approaches zero. Essentially then, the time scales of the

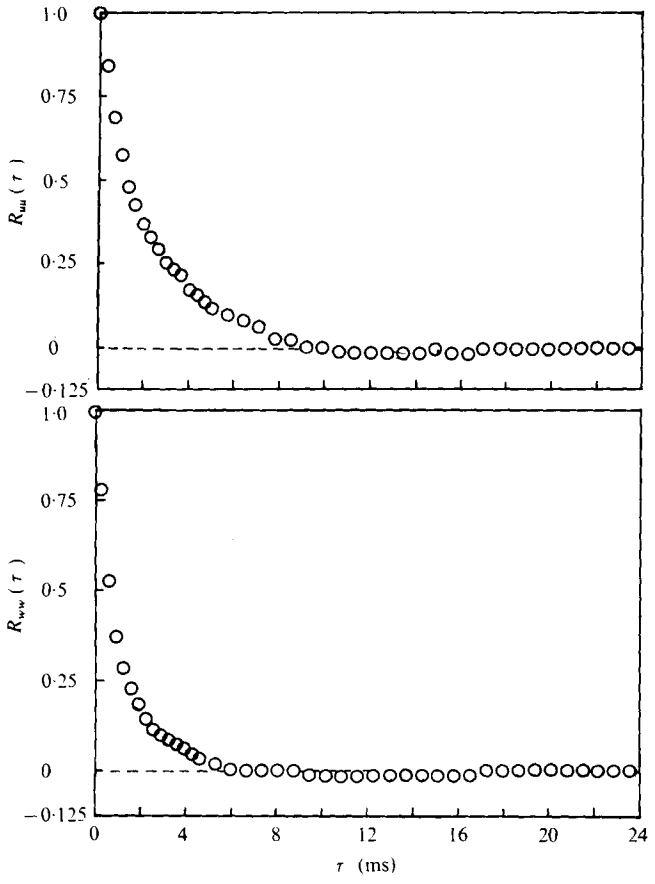


FIGURE 7. Velocity autocorrelations. $I_u = 15$ mm, $I_w = 8$ mm.

temperature fluctuations and the heat-transport correlation are larger than that of the vertical velocity component. At large values of $\tau$, however, the correlations become slightly negative. Indeed this is required by the continuity equation (Batchelor 1970) for the $w$ component of the velocity. The $u$- and $w$-component autocorrelations are compared in figure 7. From these, it is seen that the ratio of the integral scales is close to 2 as expected for isotropic turbulence.

The one-dimensional spectra of the $u$ and $w$ components of the velocity at

$$x/M = 17{\cdot}7, \quad z/M = 0$$

with the heaters in the grid turned on and off are presented in figure 8. Since the spectrum of each component remains unchanged when the grid is heated, it can be concluded that the temperature in our experiment does not alter the dynamics of the flow, thus behaving as a passive attribute. Measurements of the intensities of the velocity components with and without heating gave rise to the same conclusion. As the mean temperature gradient in the present experiments is a stable one, its effect would be to inhibit the vertical motions provided that the gradient was strong enough to influence the velocity field through a buoyancy term in the momentum equation. A criterion for the importance of buoyancy effects is the ratio of the buoyant forces to

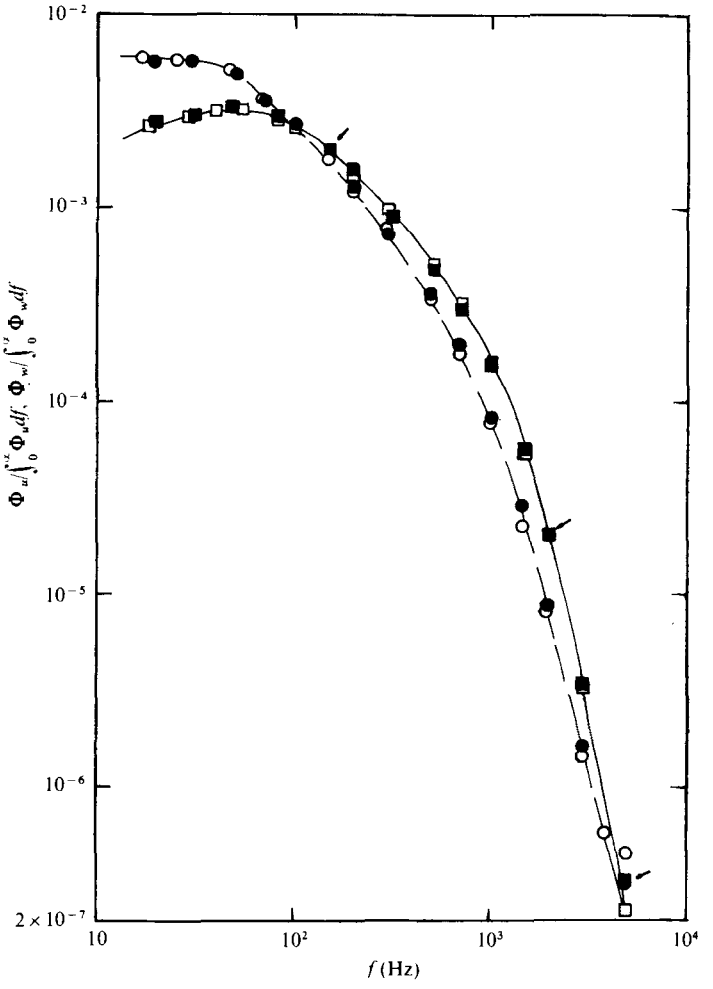


FIGURE 8. Frequency spectra of $u$ and $w$ with and without heating. ○, $u$ (heat on); ●, $u$ (cold); □, $w$ (heat on); ■, $w$ (cold); →, coincident.

the inertia forces. Taking the meash length $M$ as a characteritic length scale, we can write this ratio as

$$\frac{gMd\theta/dz}{\overline{T}}\frac{\overline{U}^2}{M},$$

which in our case is $0{\cdot}18\times10^{-4}$. This is indeed consistent with the experimental observation with regard to the spectra.

In figure 9 the frequency spectrum of $\theta$ is compared with those of $u$ and $w$ and in figure 10 the three-dimensional spectra $E(k)$ and $E_\theta(k)$ are presented. A direct differentiation procedure would lead to considerable errors since the spectra vary by several decades in the entire $k$ range. Hence the equivalent logarithmic differentiation procedure due to Uberoi (1963) was used to compute $E(k)$ and $E_\theta(k)$. The viscous dissipation rate is

$$\epsilon = 2\nu\overline{s_{ij}s_{ij}},$$

where

$$s_{ij} = \frac{1}{2}\left(\frac{\partial u_i}{\partial x_j}+\frac{\partial u_j}{\partial x_i}\right);$$

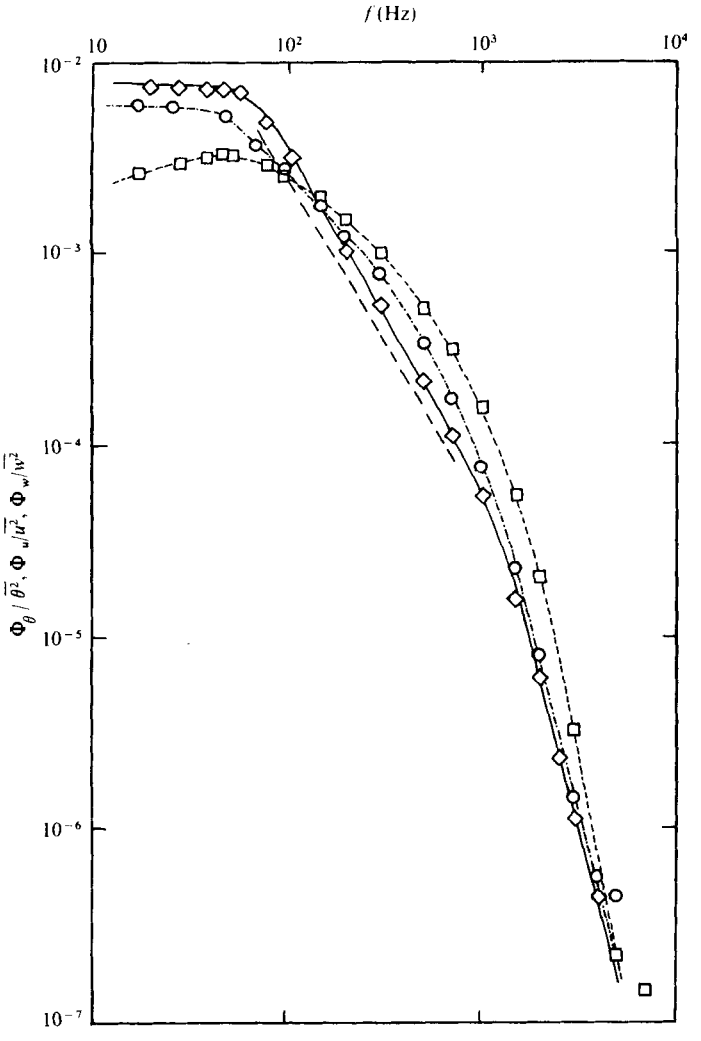


FIGURE 9. Spectra of $u$, $w$ and $\theta$. ◇, $\Phi_\theta/\overline{\theta^2}$; ○, $\Phi_u/\overline{u^2}$; □, $\Phi_w/\overline{w^2}$.

similarly, the rate of dissipation of the temperature fluctuations by the molecular diffusivity, denoted by $\epsilon_\theta$, is defined as

$$\epsilon_\theta = 2\alpha \overline{\frac{\partial\theta}{\partial x_j}\frac{\partial\theta}{\partial x_j}}.$$

These are related to $E(k)$ and $E_\theta(k)$ in the following manner:

$$\epsilon = 2\nu \int_0^\infty k^2 E(k)\,dk, \quad \epsilon_\theta = 2\alpha \int_0^\infty k^2 E_\theta(k)\,dk. \tag{22}$$

The integrands of (22) are plotted in figure 11.

A striking feature of figure 9 is that while neither of the velocity components exhibits a power-law relation of the kind $k^{-\frac{5}{3}}$ there is a distinct region (about one decade) in which the temperature spectrum obeys this law. For the existence of an inertial subrange in which $E(k) \sim k^{-\frac{5}{3}}$, it is required that $Re_\lambda^{\frac{3}{2}} \gg 1$, a condition which is clearly not

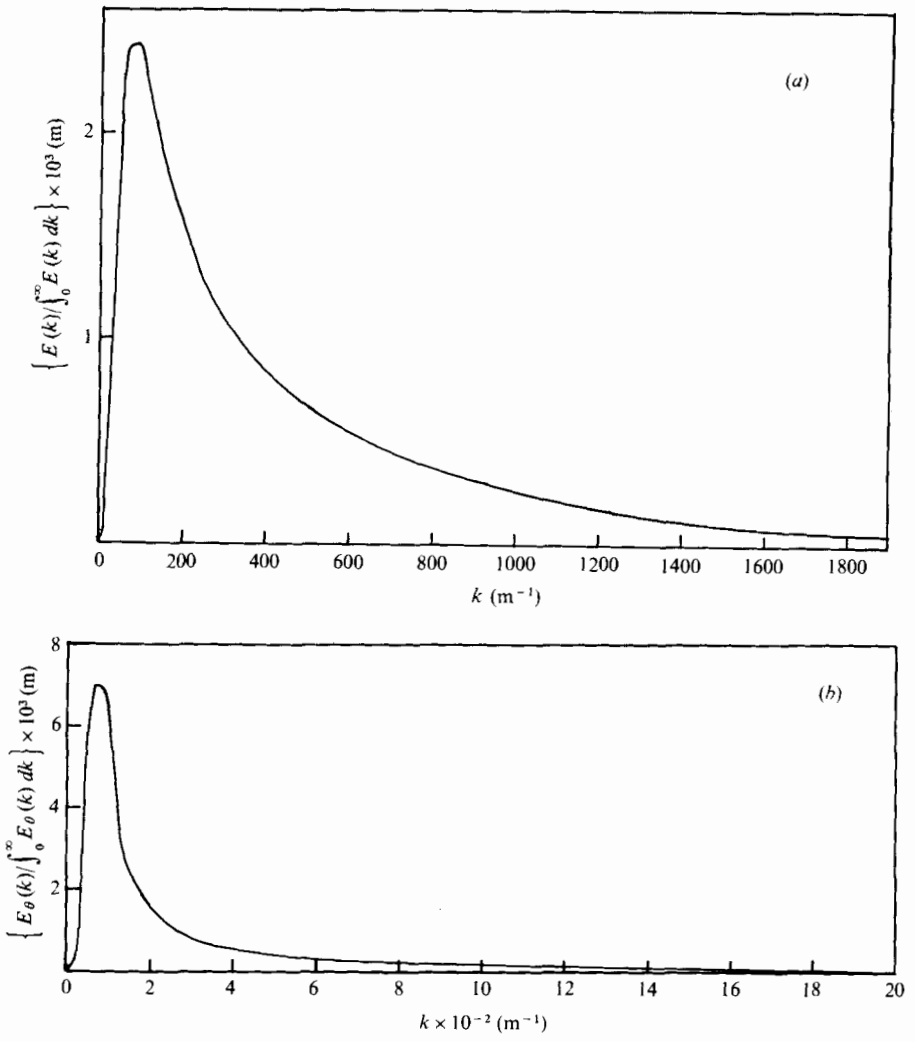


FIGURE 10. (*a*) Three-dimensional energy spectrum of velocity and (*b*) three-dimensional spectrum of temperature. $x/M = 17{\cdot}7$, $z/M = 0$.

satisfied in our experiment as is evident from the velocity spectra. Under these circumstances the apparent convective range of the temperature spectrum may be regarded as a mere coincidence. But this could be dismissed in view of the results of Yeh (1971) and Sepri (1971), which show a similar convective range for the temperature spectrum in a low Reynolds number turbulence produced by a uniformly heated grid. In high Reynolds number turbulent flows of fluids having a Prandtl number of order unity, the inertial and convective subranges can be expected to coexist. According to the classical arguments (Corrsin 1951*b*; Batchelor 1959), if a universal equilibrium exists and if in addition the molecular diffusivity is small enough to have negligible effect on a portion of the equilibrium range, then the temperature spectrum must have the following functional form within this subrange:

$$E_\theta(k) = f(\epsilon, \epsilon_\theta, \nu). \tag{23}$$

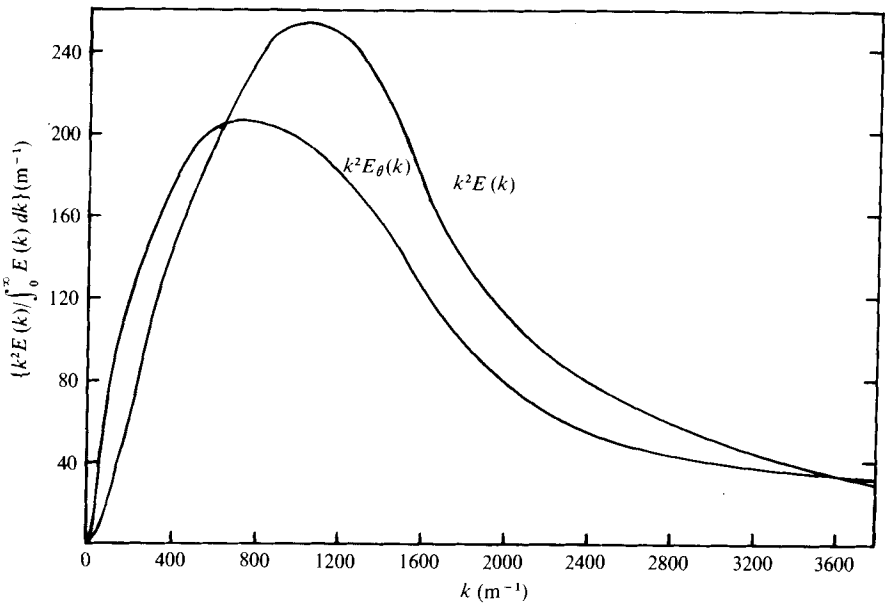


FIGURE 11. Dissipation spectra of velocity and temperature. $x/M = 17{\cdot}7$, $z/M = 0$.

Furthermore, if the Reynolds number is so large that in addition to the molecular diffusivity the viscosity is also unimportant for at least a part of the above subrange, then by dimensional reasoning the form of the temperature spectrum is given by

$$E_\theta(k) = A\epsilon^{-\frac{1}{3}}\epsilon_\theta k^{-\frac{5}{3}}, \tag{24}$$

where $A$ is a dimensionless constant. Obviously, then, in order to have (24) we must assume a large Reynolds number in addition to invoking a universal-equilibrium hypothesis if we retain the same formal reasoning as Corrsin (1951*b*) and Batchelor (1959). On the other hand, in view of the presence of a convective range and in spite of a low Reynolds number in three experiments, it appears that we may relax the requirements for the existence of the convective range.

Returning to figure 10, it is observed that the maximum value of $E(k)$ occurs near $k = 80\,\mathrm{m}^{-1}$ and that of $E_\theta(k)$ near $70\ \mathrm{m}^{-1}$. These correspond to lengths of 1·25 and 1·43 cm, respectively, and are indicative of the length scales of the energy-containing eddies for the two fields. As would be expected, they lie between the diameter of the grid rods and heaters (0·95 cm) and the mesh length of the grid (3·81 cm). In contrast to the locations of the maxima of $E(k)$ and $E_\theta(k)$, those of $k^2E(k)$ and $k^2E_\theta(k)$ are well separated, the former being at $1050\ \mathrm{m}^{-1}$ and the latter at $760\ \mathrm{m}^{-1}$.

The large-scale eddies are the most effective in transporting heat, momentum, etc. and the filtered correlation $\overline{w_f\theta_f}$ presented in figure 12 clearly illustrates this point. The results obtained by the two different methods explained earlier are close to each other except at high frequencies, where the discrepancy seems to be due to noise. At the very low frequencies the errors may be considerable owing to small effective averaging times. A large part of the heat transport is contributed by the large-scale eddies. In fact, up to 60 % of the transport is carried out below 100 Hz (figure 13). This frequency corresponds roughly to a length scale of 1·3 cm, which is of the order of the

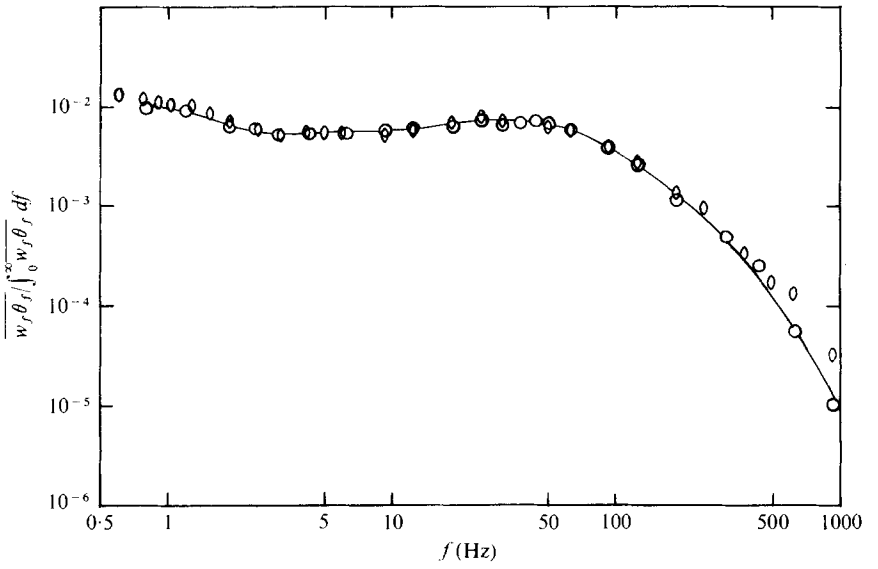


FIGURE 12. Filtered correlation of $w$ and $\theta$. $x/M = 43{\cdot}2$, $z/M = 0$. ○, two wave analysers; ○, single wave analyser.

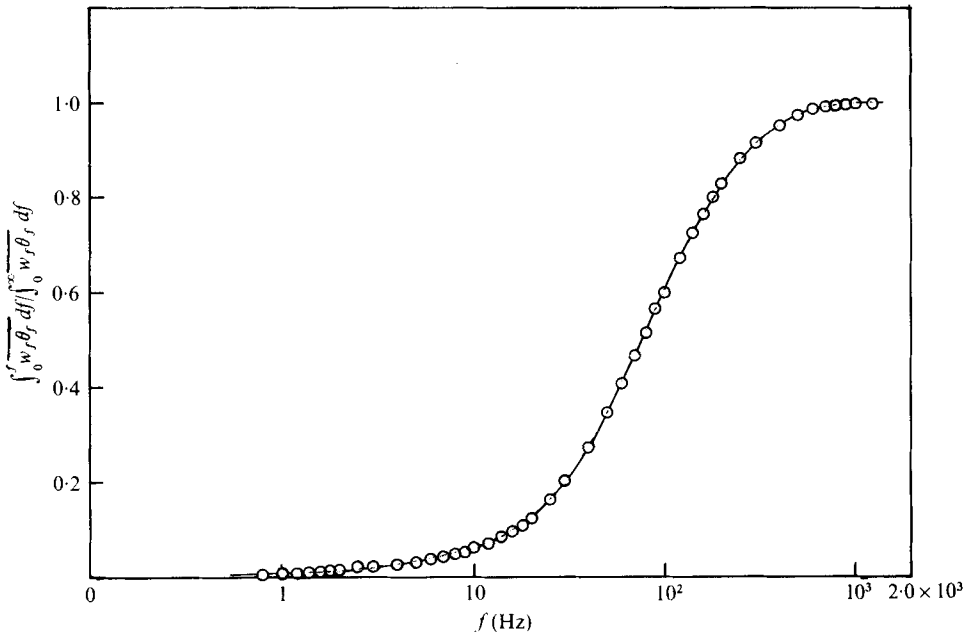


FIGURE 13. Filtered correlation integral. $x/M = 43{\cdot}2$, $z/M = 0$.

integral scale of the turbulence. The location of the peak in the filtered correlation (figure 12) around 35 Hz corresponds to the mesh length of the grid. These measurements lend support to the argument put forward in § 2 with regard to the success of Corrsin's theory in predicting the correct asymptotic behaviour of $\overline{w\theta}$. Consequently, as seen from figures 12 and 13, the neglect of molecular diffusivity in the context of the

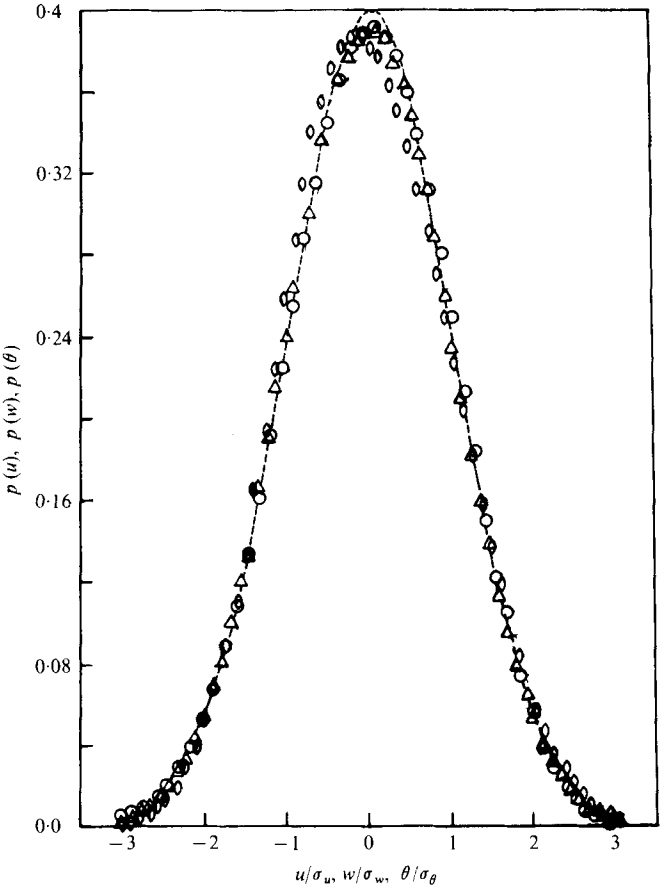


FIGURE 14. Marginal probability density functions. △, $p(u)$; ○, $p(w)$; ○, $p(\theta)$; ---, normal distribution.

evolution of $\overline{w\theta}$ is not a serious omission as its influence is unlikely to be felt at such low frequencies.

The marginal probability density function (pdf) $p(.)$ of a random process $x(t)$ is an important quantity containing all the information for the marginal moments. The pdf's of $u$, $w$ and $\theta$ at $x/M = 43{\cdot}2, z/M = 0$, which are typical of measurements made at several locations, are presented in figure 14. For ease of comparison, the variables have been standardized by dividing by their respective standard deviations. Also shown in the same figure is the pdf of a standard normal random variable given by

$$p_n(x) = (2\pi)^{-\frac{1}{2}} \exp(-\tfrac{1}{2}x^2). \tag{25}$$

Several decades of experimental research in turbulence have firmly established that the marginal pdf's of the turbulent velocity components in a grid-generated turbulence are very nearly normal, as Batchelor (1970) indicated that they would be if the central limit theorem in some form is invoked. Isotropy would require the pdf of the velocity components to be symmetrical in order to satisfy invariance to arbitrary rotations. This, however, is not required for a scalar like temperature, so that odd-order moments need not be zero for an isotropic temperature field. Each of the velocity components

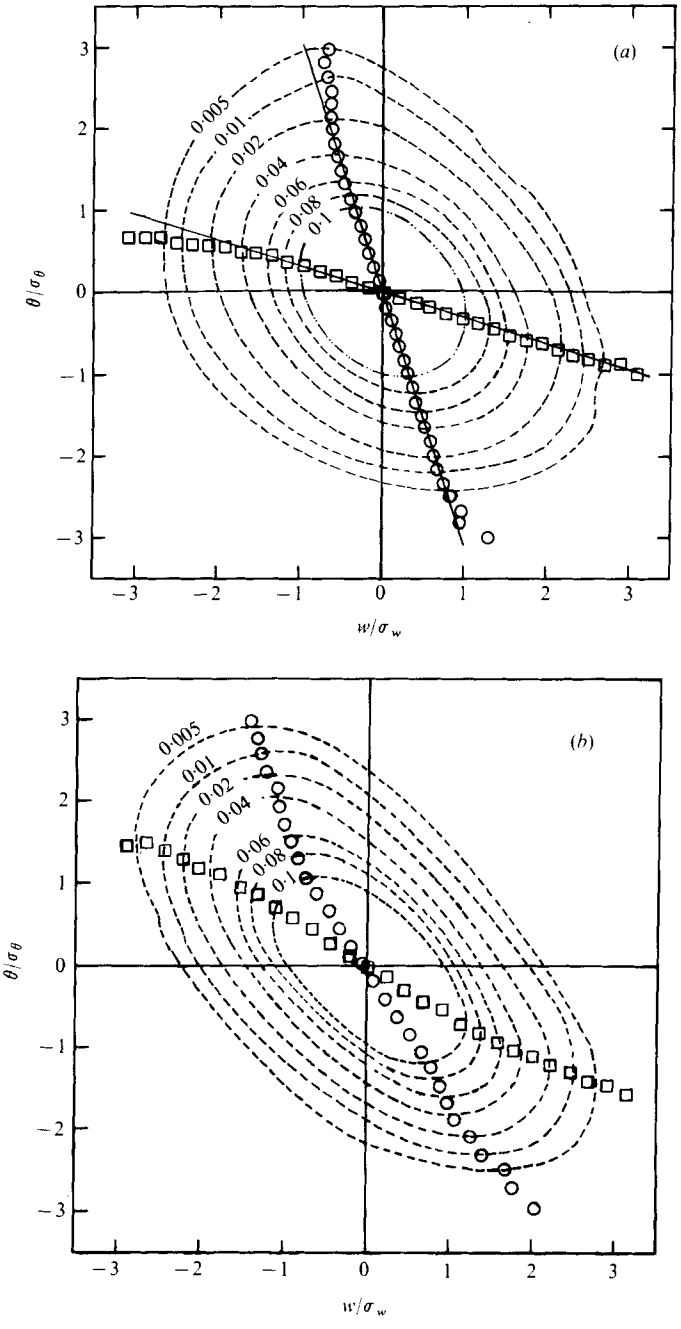


FIGURES 15 (*a*, *b*). For legend see opposite page.

exhibits near normality in contrast to the temperature, which is positively skewed. Yeh (1971) found that $p(\theta)$ was also nearly normal in a uniformly heated grid turbulence. Thus the large positive skewness of the temperature is an interesting feature of the present experiments.

Any statistical approach to the problem of heat transport by turbulence involves the

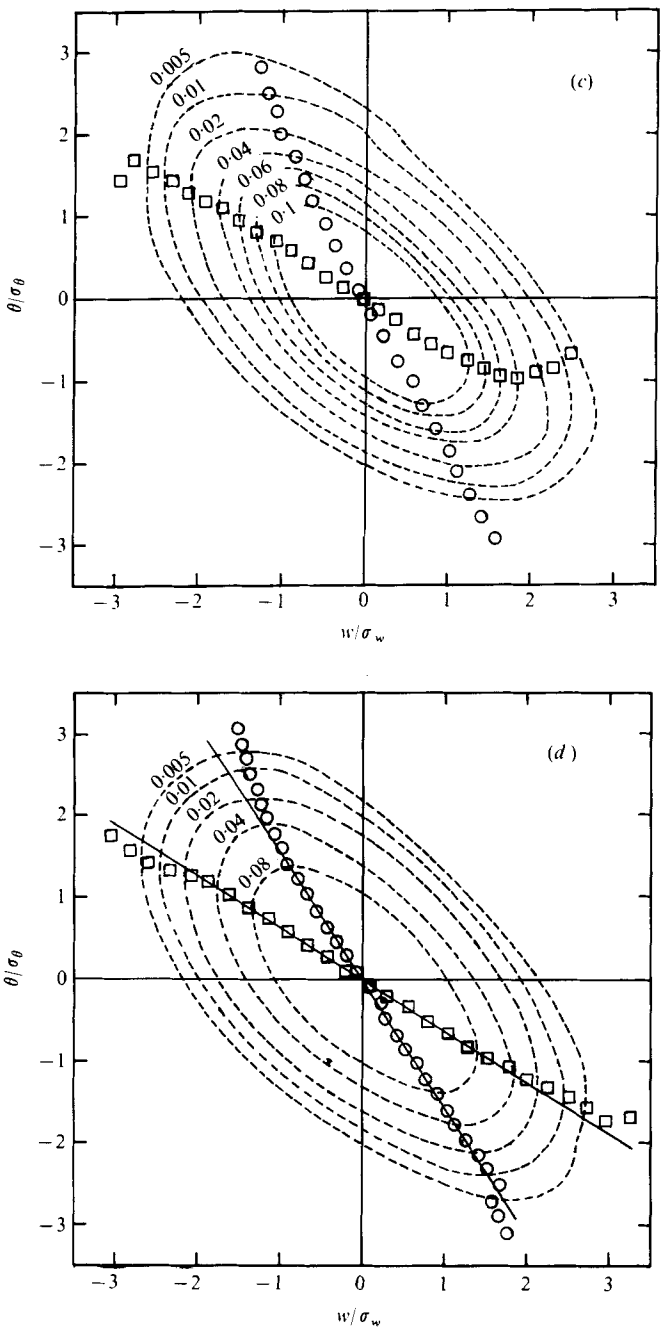


FIGURE 15. Joint pdf of $w$ and $\theta$ at $z/M = 0$. ○, $\overline{w}_c$; □, $\overline{\theta}_c$. Here $\overline{w}_c$ and $\overline{\theta}_c$ are the conditioned means. (*a*) $x/M = 17{\cdot}7$; –···–, normal distribution. (*b*) $x/M = 43{\cdot}2$. (*c*) $x/M = 49{\cdot}2$. (*d*) $x/M = 55{\cdot}2$.

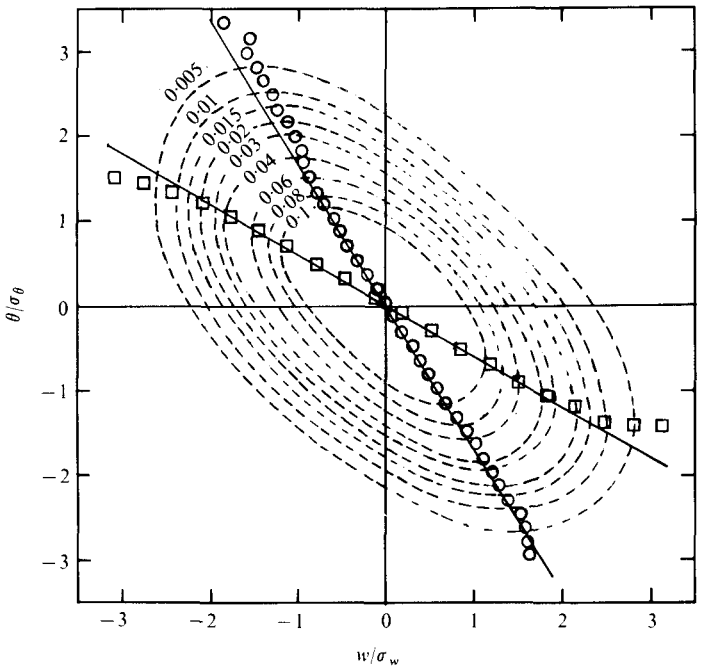


FIGURE 16. Joint pdf of $w$ and $\theta$ at $x/M = 49{\cdot}2$, $z/M = -2{\cdot}0$. Symbols as in figure 15.

joint probability structure of the velocity and temperature fields in some form or other. However very little experimental information is currently available in this area. Here we are particularly interested in the joint probability density function of the vertical component of the velocity and the temperature. Although $p(w, \theta)$ was obtained for several locations, only the measurements for four locations along the longitudinal axis of the tunnel and one location at $z/M = -2{\cdot}0$ are presented here. Figures 15 ($a$)–($d$) show $p(w, \theta)$ for $x/M = 17{\cdot}7$, $43{\cdot}2$, $49{\cdot}2$ and $55{\cdot}2$ and $z/M = 0$ and figure 16 shows this probability density function at $x/M = 49{\cdot}2$ and $z/M = -2{\cdot}0$.

Among several interesting features which emerge from the equi-probability curves, an asymmetry can be observed about the line $\theta = 0$ for the axial locations. The skewness of the temperature exerts a strong influence on the joint probability density for the fluctuations with large amplitudes. Whereas the bounding values of $w$ are nearly symmetrical for each of the curves, the positive bound for $\theta$ is greater than the negative one. Since $\theta$ is positively skewed, large positive fluctuations (about the mean) are more probable than large negative fluctuations and this is directly reflected in the joint probability distribution. It is also apparent that this influence of the skewness decreases for increasing values of $p(w, \theta)$, which correspond to smaller fluctuations about the mean.

One of the important conclusions we can draw from these curves is that the assumption of a joint normal pdf given by

$$p_{n,w\theta}(w, \theta) = (2\pi)^{-1}(1-\rho^2)^{-\frac{1}{2}} \exp\{-[2(1-\rho^2)]^{-1}(w^2 - 2\rho w\theta + \theta^2)\}, \qquad (26)$$

where $\rho$ is the correlation coefficient of $w$ and $\theta$, is not a uniformly good approximation. The equi-probability contours for (26) are a family of concentric ellipses. To avoid a

profusion of contours in each figure and also since the deviation from a smooth ellipse is easy to detect from the curves, we have shown only one contour for the joint normal pdf with the measured value of the correlation coefficient. The most pronounced deviations from the joint normal ellipses occur for small values of $p_{w\theta}$, which correspond to relatively large fluctuations (of the order of 2 or 3 standard deviations) for one or both the variables. As the value of $p_{w\theta}$ increases, the contours gradually approach the joint normal distribution. Thus it is the large amplitude fluctuations which display noticeable non-normality just as in the case of the marginal distribution, where the skewness gets its greatest contribution from the tails of the distribution.

Although similar joint probability measurements in a grid turbulence with a uniform gradient are not found in the literature, it is helpful to compare the few available measurements (some made under vastly differing circumstances) with our results. In a series of papers Frenkiel & Klebanoff (1965, 1967*a*, *b*, 1973) have contributed a wealth of information on the joint statistics of the velocity fields in grid turbulence and in turbulent boundary layers. In the case of the grid turbulence they found that the joint probability density of the longitudinal components of the velocity at two locations separated in the transverse direction but on the same plane normal to the mean flow direction clearly departed from the joint normal law. There were noticeable irregularities in the equi-probability curves for $p = 0{\cdot}005$ and $0{\cdot}02$. In the latest study (1973), the joint densities of the longitudinal velocity were presented at $y/\delta = 0{\cdot}27$ in a turbulent boundary layer. Instead of using two probes, Frenkiel & Klebanoff took the signal from a single probe and delayed it by a certain time to give the second signal, thus obtaining the joint density of the velocity at two different times but at the same spatial position. Comparison with similar results from a grid turbulence with approximately the same value of the correlation coefficient showed that, while neither of the measured distributions followed the normal distribution exactly, the distribution for the grid turbulence was more symmetric and closer to the normal distribution. Use of the non-normal Gram–Charlier expansion proved to be more successful than the normal law in approximating the measured distributions.

Recent measurements in a round heated jet (Venkataramani, Tutu & Chevray 1975) showed that, while $p(u, v)$ and $p(v, \theta)$ were nearly normal at the centre-line of the jet, $p(u, \theta)$ was asymmetrical and even a non-normal Gram–Charlier distribution involving cumulants of up to the fourth order achieved only very little success in approximating $p(u, \theta)$. Joint densities at 1 and 1·89 diameters away from the centreline indicated a trend of increasing departure from normality with increasing distance from the axis. A striking contrast with the present results is offered by their measurements at 1·89 diameters. At this position, where the intermittency factor was 0·6, both $p(u, v)$ and $p(v, \theta)$ exhibit enormous deviations from the normal law. Interpretation of the joint pdf results with such a high intensity of turbulence as was encountered at $r/d = 1{\cdot}89$ in the heated-jet measurements requires caution since rectification effects of the hot wires are very pronounced for cross-wire anemometry in high intensity turbulence (Tutu & Chevray 1975). The rectification essentially introduces bounds on the amplitudes in the $u$, $v$ plane like those left unexplained in Ribeiro & Whitelaw (1975). In spite of the scatter in the data owing to intermittency and high intensity of the turbulence, it was clear that the assumption of joint normality was a serious misrepresentation of the actual statistical features of the flow.

Yeh (1971) reported that $p(u, \theta)$ in a uniformly heated grid turbulence was closely

approximated by a bivariate-normal distribution with a correlation coefficient of $-0{\cdot}155$ even though the measured value of the coefficient was $-0{\cdot}1476$. Among the various investigations just cited, Yeh's experiments bear the closest resemblance to the present work. The only significant difference is the absence of a temperature gradient in his study. Thus it appears that the introduction of a mean temperature gradient, even if it is uniform, distorts the joint statistical structure of the velocity and temperature. The close interrelation between the departure from joint normality and the local skewness of the temperature distribution is evident from figure 16, which shows $p_{w\theta}(w, \theta)$ at $x/M = 49{\cdot}2, z/M = -2{\cdot}0$, where the skewness of the temperature is small and the joint distribution follows the normal law better than at, say, $x/M = 17{\cdot}7$, $z/M = 0$.

The conditional mean of a random variable $x$ given that another random variable has taken the value $y = y_0$ is given by

$$E(x|y = y_0) = \int_{-\infty}^{\infty} xp(x|y = y_0)\,dx, \tag{27}$$

where $p(x|y = y_0)$ is the conditional pdf. For a bivariate-normal distribution, the conditional means are linear in the values of the conditioned variable and have slopes equal to $\rho$ and $\rho^{-1}$. It is a little surprising, then, that the conditional means in the present experiments follow this behaviour although the distributions themselves are not normal. The reason perhaps lies in the fact that the major contribution to the integral comes from the inner regions of the $p_{w\theta}(w, \theta)$ contours, where the distribution is not far from the normal. For large values of the conditioned variable, however, this is no longer true and consequently the deviations from the straight lines are appreciable. Another interesting facet of the distributions is revealed by figures 17 (*a*), (*b*) and (*c*), which represent the cross-sections of the $p_{w\theta}(w, \theta)$ surface formed by planes corresponding to different constant values of $\theta$. Each of these curves representing the joint pdf differs from the conditional pdf of $p(w/\theta)$ only by a normalization constant. The conditional pdf of $w$ given $\theta$ is remarkably close to a normal distribution.

In view of the well-known difficulties associated with the moment formulation, a new closure method is emerging. This approach yields a hierarchy of equations involving the probability distributions (Lundgren 1967, 1972; Hill 1970; Dopazo & O'Brien 1974; Dopazo 1975). Here the closure problem is to relate the higher-order distributions to lower-order ones. In order to keep the mathematical complexities at a tractable level, a theoretically convenient approach is to invoke the normality assumption at some stage of the development. Available results indicate that this method is more promising than the conventional moment formulation. Lundgren (1972), for instance, was able to derive the Kolmogorov inertial-subrange spectrum using a closure at the two-point distribution level. Also, his value of 1·29 for the Kolmogorov constant is remarkably close to the value of 1·44 found experimentally by Grant, Stewart & Moilliet (1962). Dopazo (1975), using a conditionally normal distribution, showed that the pdf closure could well approximate the measured marginal pdf of the temperature along the centre-line of a heated round jet. Our results indicate that a certain amount of caution is required in such closures. In the context of grid turbulence with a uniform gradient, a straightforward assumption of joint normality of $w$ and $\theta$ can be expected to be valid only at large distances from the grid and is likely to be erroneous at short distances, where the joint distribution is influenced by the presence of the gradient.

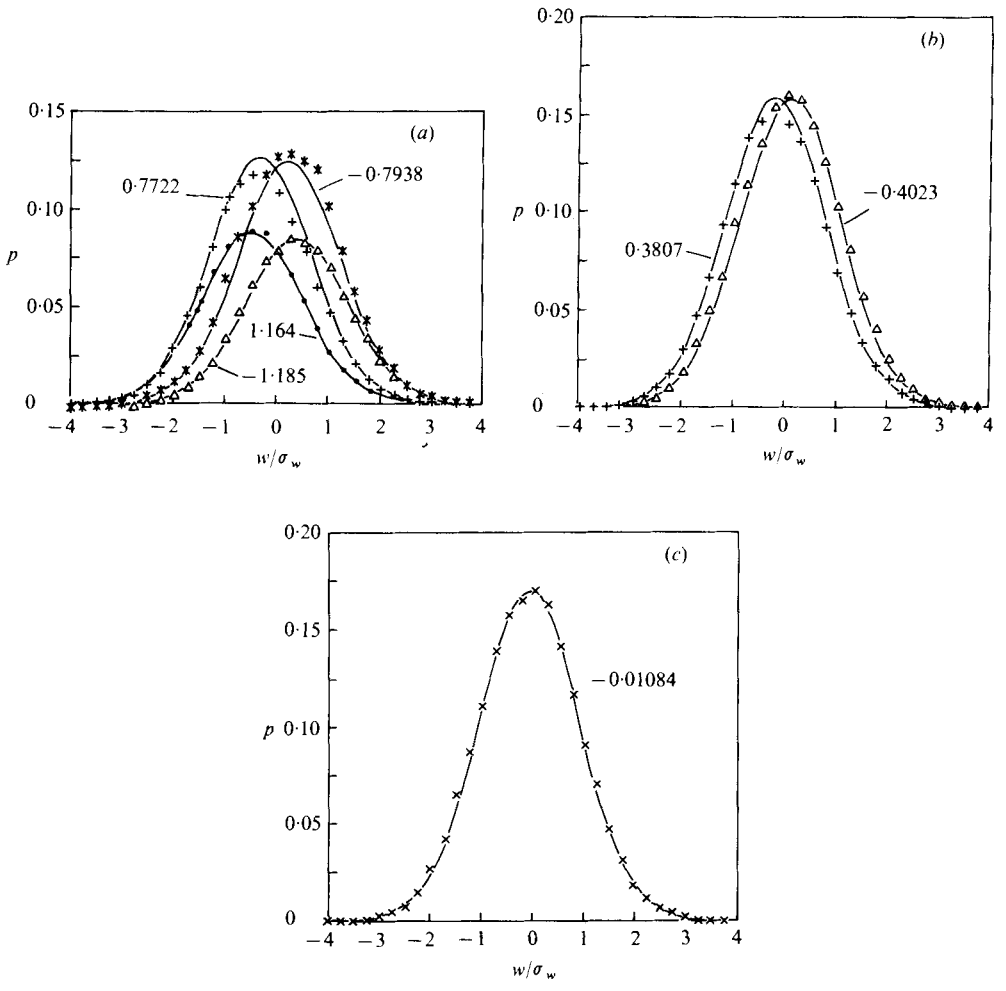


FIGURE 17. Joint pdf $p(w, \theta = \theta_0)$. (*a*) $\theta_0 = -1{\cdot}185, +1{\cdot}164, -0{\cdot}7938, +0{\cdot}7722$. (*b*) $\theta_0 = -0{\cdot}4023, +0{\cdot}3807$. (*c*) $\theta_0 = -0{\cdot}01084$. —, joint normal distribution. $x/M = 17{\cdot}7$.

On the other hand assumption of normality for the conditional expectation seems justified even for short distances.

While the marginal pdf gives an excellent first idea of the gross features of the distribution, the actual measurements of the moments of the distribution have a more direct application in various theoretical models. Obviously the odd-order moments are indicative of the symmetry of the distribution and since the even-order moments are influenced by the limiting amplitudes of the fluctuations, the third- and fifth-order moments of $\theta$ across the height of the test section at $x/M = 43{\cdot}2$ are presented in figure 18, whereas the fourth- and sixth-order moments appear separately in figure 19. Both $\overline{\theta^3}$ and $\overline{\theta^5}$ are significantly different from zero and have nearly identical shapes. That $\overline{\theta^3}$ is always positive might be surprising at first, but recalling from figure 5 that $\theta'$ is not uniform across the height but generally increases with increasing mean temperature, it can be expected on the average that a fluid particle with a large fluctuation in $\theta$ is likely to come from a

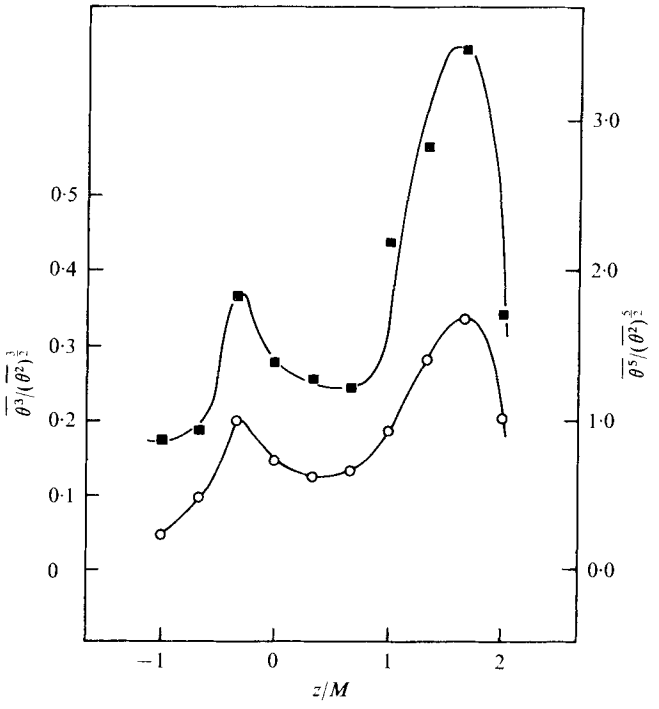


FIGURE 18. Skewness factor and normalized fifth moment of temperature at $x/M = 43{\cdot}2$. ○, $\overline{\theta^3}/(\overline{\theta^2})^{\frac{3}{2}}$; ■, $\overline{\theta^5}/(\overline{\theta^2})^{\frac{5}{2}}$.

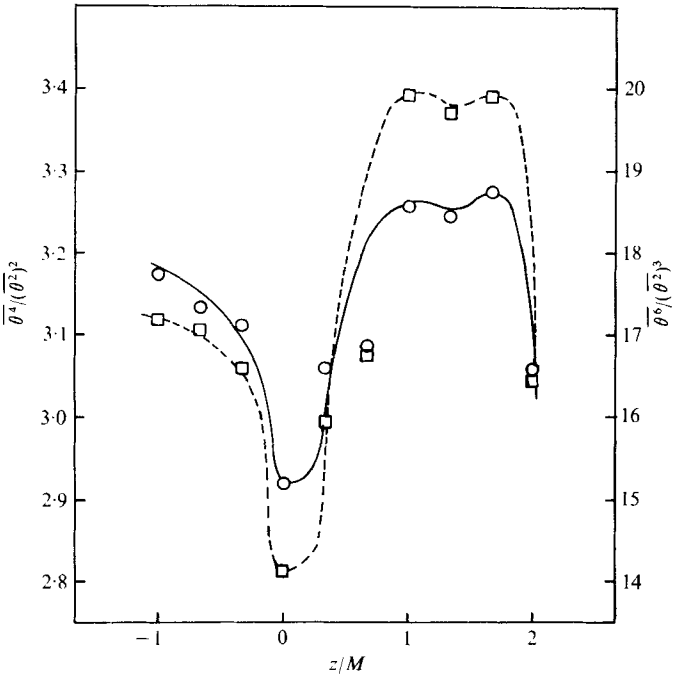


FIGURE 19. Normalized fourth and sixth moments of temperature at $x/M = 43{\cdot}2$. ○, $\overline{\theta^4}/(\overline{\theta^2})^2$; □, $\overline{\theta^6}/(\overline{\theta^2})^3$.

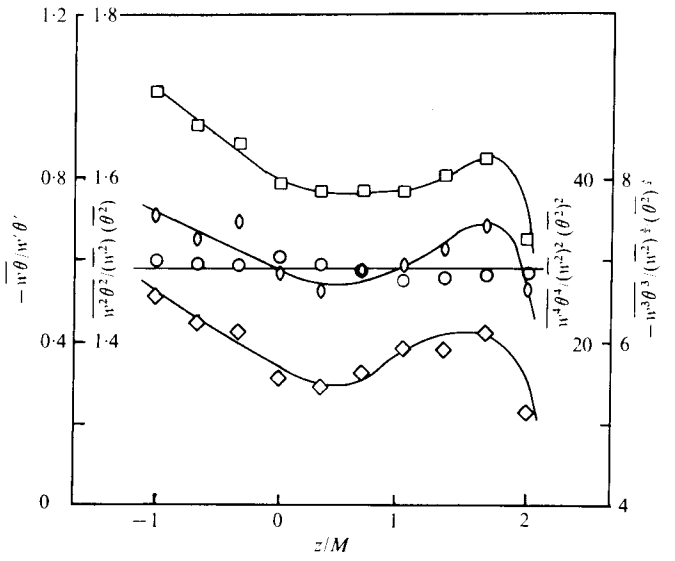


FIGURE 20. Joint moments of $w$ and $\theta$: diagonal moments at $x/M = 43{\cdot}2$. ○, $-\overline{w\theta}/w'\theta'$; □, $\overline{w^2\theta^2}/(\overline{w^2})\,(\overline{\theta^2})$; ◇, $-\overline{w^3\theta^3}/(\overline{w^2})^{\frac{3}{2}}(\overline{\theta^2})^{\frac{3}{2}}$; ○, $\overline{w^4\theta^4}/(\overline{w^2})^2(\overline{\theta^2})^2$.

region with a mean temperature larger than the local mean and conversely a small fluctuation in $\theta$ is associated with a mean temperature less than the local mean. Thus at a given spatial position the probability of encountering large positive (greater than the mean) amplitudes of the temperature fluctuations is greater than that of encountering large negative amplitudes. Therefore from this rough physical picture it follows that the temperature distribution must indeed have a positive skewness. This explanation amounts to a closure statement since the third moment of $\theta$ is related to the mean and the variance of $\theta$. The fourth and sixth moments of $\theta$ in figure 19 do not exhibit a uniform behaviour with respect to the deviation from the normal values of 3 and 15, respectively. At $z/M = 0$ they fall below these values and exceed them everywhere else. There seems to be no direct relation between the even moments and the odd moments in figure 18. An explanation similar to that for the skewness cannot be given here since an inference with regard to the specific deviation from the normal distribution would have to be made instead of just using symmetry considerations as was done for $\overline{\theta^3}$. While figure 20 gives the diagonal moments of $\overline{w^i\theta^j}$ (with $i = j$), figures 21 and 22, respectively, show selected odd and even off-diagonal moments. Diagonal moments with $i,j > 1$ are remarkably similar to each other and calculations showed that they are also nearly equal to the values obtained from a joint normal relation with the same local value of the correlation coefficient. The value of the heat-transport correlation coefficient $\overline{w\theta}/w'\theta'$ is nearly constant and has an average value of $-0{\cdot}58$.

There is a strong relationship between the marginal odd-order moments of $\theta$ and the odd-order off-diagonal joint moments. The distributions of the latter across the height are similar not only to each other but to $\overline{\theta^3}$ and $\overline{\theta^5}$ as well. For $p_{n,w\theta}(w,\theta)$ all these moments must vanish identically. From $\overline{w\theta^2}$ and $\overline{w^2\theta}$ it appears that, owing to a large contribution from the non-normal $\theta$ in $\overline{w\theta^2}$, this quantity deviates from zero more than $\overline{w^2\theta}$ does. Even-order off-diagonal moments are shown in figure 22. Although a similarity with the diagonal moments is observable, the resemblance shown in figure 5 is

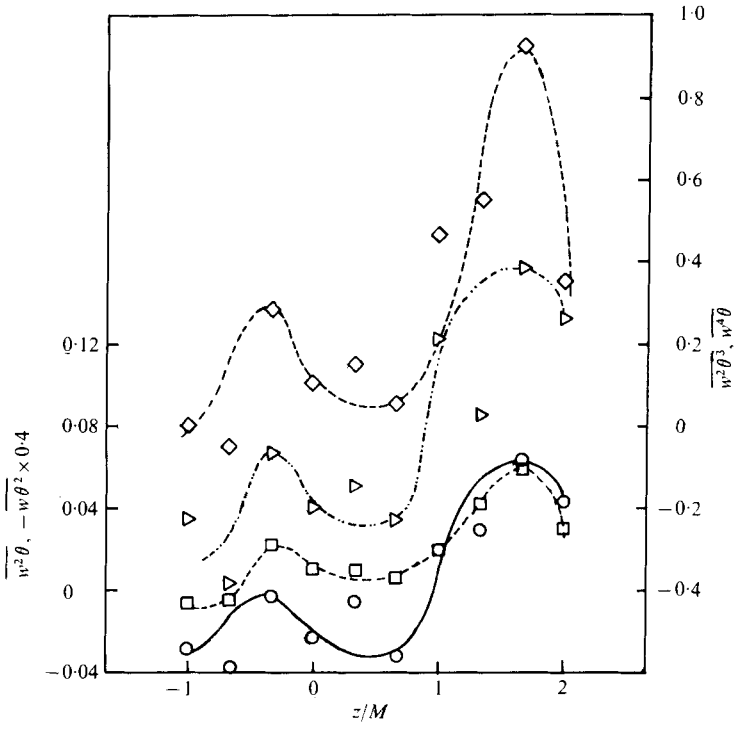


FIGURE 21. Odd-order moments at $xM = 43{\cdot}2$. ○, $\overline{w^2\theta}$; □, $-\overline{w\theta^2}$; ◇, $\overline{w^2\theta^3}$; △, $\overline{w^4\theta}$.

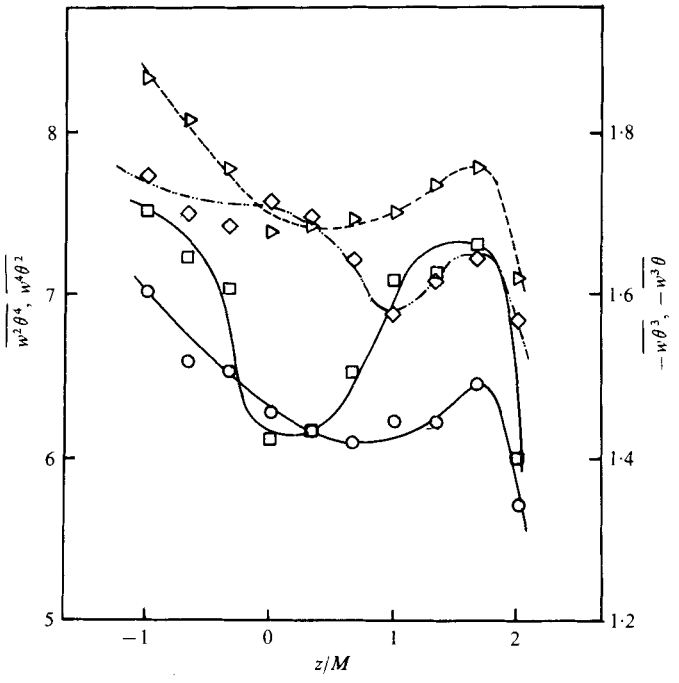


FIGURE 22. Even-order off-diagonal joint moments at $x/M = 43{\cdot}2$. ▷, $-\overline{w\theta^3}$; ◇, $-\overline{w^3\theta}$; □, $\overline{w^2\theta^4}$; ○, $\overline{w^4\theta^2}$.

| Parameter | Value |
|---|---|
| $U$ | 8·16 m/s |
| $u'/U$ | 4·05% |
| $\Delta T$ | 4·04 °C |
| $d\overline{T}/dz$ | 0·0994 °C/cm |
| $\theta'$ | 0·1633 °C |
| $\lambda_u$ | 3·02 mm |
| $Re_\lambda$ | 64·4 |
| $\eta$ | 0·19 mm |
| $\lambda_\theta$ | 1·57 mm |
| $Re_M$ | $2·01 \times 10^4$ |

TABLE 2. Flow parameters at $x/M = 17·7$, $z/M = 0$. $\lambda_u$ and $\lambda_\theta$ refer to the Taylor and Corrsin microscales, respectively. $\eta$ is the Kolmogorov microscale.

| $j$ \ $i$ | 0 | 1 | 2 | 3 | 4 |
|---|---|---|---|---|---|
| 0 | 1 | 0 | 1 | −0·05152 | 2·9972 |
| 1 | 0 | −0·3155 | −0·01719 | −0·8840 | −0·08535 |
| 2 | 1 | −0·05773 | 1·146 | −0·1376 | 3·764 |
| 3 | 0·3018 | −0·9883 | 0·2808 | −2·775 | 0·7277 |
| 4 | 3·3392 | −0·7218 | 4·225 | −1·632 | 14·28 |

TABLE 3. Joint moments $\overline{w^i\theta^j}/w'^i\theta'^j$ of $w$ and $\theta$ at $x/M = 17·7$, $z/M = 0$.

| $j$ \ $i$ | 0 | 1 | 2 | 3 | 4 |
|---|---|---|---|---|---|
| 0 | 1 | 0 | 1 | 0·04132 | 2·9852 |
| 1 | 0 | −0·6084 | −0·02381 | −1·715 | −0·2068 |
| 2 | 1 | −0·02347 | 1·593 | 0·07361 | 6·287 |
| 3 | 0·1434 | −1·674 | 0·1029 | −5·586 | −0·5829 |
| 4 | 2·9204 | −0·4084 | 6·112 | −0·2534 | 28·51 |

TABLE 4. Joint moments $\overline{w^i\theta^j}/w'^i\theta'^j$ of $w$ and $\theta$ at $x/M = 43·2$, $z/M = 0$.

| $j$ \ $i$ | 0 | 1 | 2 | 3 | 4 |
|---|---|---|---|---|---|
| 0 | 1 | 0 | 1 | 0·03170 | 2·9695 |
| 1 | 0 | −0·6146 | 0·02808 | −1·719 | −0·0007 |
| 2 | 1 | −0·1075 | 1·636 | −0·2588 | 6·270 |
| 3 | 0·2440 | −1·744 | 0·5084 | −5·686 | 1·605 |
| 4 | 2·9634 | −0·9528 | 6·410 | −2·871 | 27·67 |

TABLE 5. Joint moments $\overline{w^i\theta^j}/w'^i\theta'^j$ of $w$ and $\theta$ at $x/M = 49·2$, $z/M = 0$.

| $x/M$ | $\overline{u\theta}/u'\theta'$ |
|---|---|
| 17·7 | 0·09581 |
| 43·2 | 0·06584 |
| 49·2 | 0·06475 |

TABLE 6. Values of $\overline{u\theta}/u'\theta'$ along the tunnel axis.

not quite as strong as that between the moments in figures 21 and 18. In common with all the other moments, however, they have a peak at $z/M = 1{\cdot}67$.

It is pertinent to remark here that the variation with $z$ of the various marginal and joint moments is a reflexion of the fact that a laboratory simulation such as that described in this paper departs from the ideal problem in that, while introducing a uniform mean temperature gradient, the grid simultaneously gives rise to a non-uniform distribution of $\theta'$ in the vertical direction.

## 5. Concluding remarks

When a mean temperature profile varying linearly with height is imposed in a grid-generated turbulence, the profile remains linear with the same slope at all downstream locations in accordance with the simple and elegant theory of Corrsin. This had also been previously shown by others. We observed here that the presence of the decay of the kinetic energy in a grid turbulence does not alter this conclusion although it was originally proposed for a non-decaying, homogeneous turbulence.

A rather serious shortcoming of the theory, namely the neglect of molecular diffusion, was also investigated. While the inclusion of the molecular diffusivity does not affect the evolution of the mean temperature profile, it does lead to the physically reasonable result that the 'energy' of the temperature fluctuations cannot increase indefinitely as Corrsin's theory suggests. The present experiments also indicate this trend.

Examination of the statistical structure of the velocity and temperature fields reveals that the probability distribution of the temperature is everywhere positively skewed in contrast with those of the velocity components, which are symmetrical and nearly normal. This peculiar feature seems to be due to the introduction of a gradient in the mean temperature at the grid plane, which in turn introduces inhomogeneity in the temperature fluctuations. The skewness in the temperature distribution is reflected in the joint statistical structure of the vertical velocity and temperature. In this regard, the assumption of joint normality for the fields involved in the transport must be viewed with caution inasmuch as the departure from joint normality is considerable even in the simplest transport case considered here. On the other hand, the experimental results suggest that the normality assumption for the conditional expectations is justified.

We are indebted to Professor E. E. O'Brien and Professor A. Okubo for critical comments and valuable suggestions. Thanks are due to the National Science Foundation for financial support at the start of this study under Grant KO40738. Support from the Direction Générale à la Recherche Scientifique et Technique, while the senior author was a Visiting Professor at the Fluid Mechanics Laboratory of the Ecole Centrale de Lyon, is gratefully acknowledged. Some of the material covered in this paper was presented orally at the New York meeting of the American Institute of Chemical Engineers on 16 November 1977.

## REFERENCES


ALEXOPOULOUS, C. C. & KEFFER, J. F. 1971 *Phys. Fluids* **14**, 216.

BATCHELOR, G. K. 1959 *J. Fluid Mech.* **5**, 113.

BATCHELOR, G. K. 1970 *The Theory of Homogeneous Turbulence.* Cambridge University Press.

BATCHELOR, G. K., HOWELLS, I. D. & TOWNSEND, A. A. 1959 *J. Fluid Mech.* **5**, 134.

CHAMPAGNE, F. H., HARRIS, V. G. & CORRSIN, S. 1970 *J. Fluid Mech.* **41**, 81.

CHEVRAY, R. & TUTU, N. K. 1972 *Rev. Sci. Instr.* **43**, 1417.

CHEVRAY, R. & VENKATARAMANI, K. S. 1977 Submitted for publication.

COMTE-BELLOT, G. & CORRSIN, S. 1966 *J. Fluid Mech.* **25**, 657.

COMTE-BELLOT, G. & CORRSIN, S. 1970 *J. Fluid Mech.* **48**, 273.

CORRSIN, S. 1951*a* *J. Aero. Sci.* **18**, 417.

CORRSIN, S. 1951*b* *J. Appl. Phys.* **22**, 469.

CORRSIN, S. 1952 *J. Appl. Phys.* **23**, 113.

CORRSIN, S. 1972 *Phys. Fluids* **15**, 986.

DOPAZO, C. 1975 *Phys. Fluids* **18**, 397.

DOPAZO, C. & O'BRIEN, E. E. 1974 *Acta Astronautica* **1**, 1239.

FRENKIEL, F. N. & KLEBANOFF, P. S. 1965 *Phys. Fluids* **8**, 2291.

FRENKIEL, F. N. & KLEBANOFF, P. S. 1967*a* *Phys. Fluids* **10**, 507.

FRENKIEL, F. N. & KLEBANOFF, P. S. 1967*b* *Phys. Fluids* **10**, 1737.

FRENKIEL, F. N. & KLEBANOFF, P. S. 1973 *Phys. Fluids* **16**, 725.

GRANT, H. L. & NISBET, I. C. T. 1957 *J. Fluid Mech.* **2**, 263.

GRANT, H. L., STEWART, R. W. & MOILLIET, A. 1962 *J. Fluid Mech.* **12**, 241.

HILL, J. C. 1970 *Phys. Fluids* **13**, 1394.

KISTLER, A. L. & VREBALOVICH, T. 1966 *J. Fluid Mech.* **26**, 37.

LUNDGREN, T. S. 1967 *Phys. Fluids* **10**, 969.

LUNDGREN, T. S. 1972 *Proc. Symp. Statistical Models & Turbulence, San Diego*, p. 70. Springer.

MILLS, R. R. & CORRSIN, S. 1959 *N.A.S.A. Memo.* no. 5-5-59W.

MILLS, R. R., KISTLER, A. L., O'BRIEN, V. & CORRSIN, S. 1958 *N.A.C.A. Tech. Note* no. 4288.

OKUBO, A. 1967 *Phys. Fluids Suppl.* **10**, S72.

RIBEIRO, M. M. & WHITELAW, J. H. 1975 *J. Fluid Mech.* **70**, 1.

SAFFMAN, P. G. 1960 *J. Fluid Mech.* **8**, 273.

SEPRI, P. 1971 Ph.D. dissertation, University of California, San Diego.

TAYLOR, G. I. 1921 *Proc. Lond. Math. Soc. Ser.* 2, **20**, 196.

TENNEKES, H. & LUMLEY, J. L. 1972 *A First Course in Turbulence.* M.I.T. Press.

TUTU, N. K. 1976 Ph.D. dissertation, State University of New York, Stony Brook.

TUTU, N. K. & CHEVRAY, R. 1975 *J. Fluid Mech.* **71**, 785.

UBEROI, M. S. 1963 *Phys. Fluids* **6**, 1048.

UBEROI, M. S. & WALLIS, S. 1966 *J. Fluid Mech.* **24**, 539.

VENKATARAMANI, K. S. 1977 Ph.D. dissertation, State University of New York, Stony Brook.

VENKATARAMANI, K. S. & CHEVRAY, R. 1977 In preparation.

VENKATARAMANI, K. S., TUTU, N. K. & CHEVRAY, R. 1975 *Phys. Fluids* **18**, 1413.

WISKIND, H. K. 1962 *J. Geophys. Res.* **67**, 3033.

WYNGAARD, J. 1971 *J. Fluid Mech.* **48**, 763.

YEH, T. 1971 Ph.D. dissertation, University of California, San Diego.